An Electron Acceptor Challenging Fullerenes for Efficient Polymer Solar Cells

*Yuze Lin, Jiayu Wang, Zhi-Guo Zhang, Huitao Bai, Yongfang Li, Daoben Zhu, and Xiaowei Zhan**

Solution-processed bulk heterojunction (BHJ)[1] polymer solar cells (PSCs) with low-cost, light-weight, and flexibility advantages are a cost-effective alternative for utilizing solar energy.[2–4] Over the last three years, PSCs have seen dramatic developments in power conversion efficiencies (PCEs) of up to 9%–10%,[5,6] having benefited from the development of new electron-donor polymers that exhibit improved properties, such as better spectral sensitivity, enhanced hole transport, and favorably tuned energy levels that match well with those of existing acceptors. In practice, the electron acceptors are as important as the electron donors for high-performance PSCs. However, the development of electron-acceptor materials has lagged far behind that of donor materials. Fullerenes and their derivatives have been the dominant electron acceptors because of their high electron mobility even in blended films, high electron affinity, and isotropic charge transport.[7] Overcoming the shortcomings of fullerenes, such as weak absorption in the visible spectral region and limited energy level variability, remains an incentive to develop alternative electron acceptors. In the last two years, considerable efforts have been dedicated to the development of non-fullerene acceptors,[8–10] and fullerene-free PSCs have shown PCEs of up to 4–5.9%.[11–17] Non-fullerene acceptors are still in their infancy compared to fullerene-based acceptors.

When new electron acceptors for PSCs are being designed, basic properties, such as energy levels, charge transport, and absorption, should be first considered. Aromatic fused rings have been widely applied in the construction of high-mobility organic semiconductors, because the extended conjugation in fused rings is beneficial to forming effective interchain π–π overlaps and enhancing intermolecular charge transport. Fused ring–based semiconductors, such as pentacene and rubrene, have shown very high charge mobilities, even exceeding 20 cm^2 V^{-1} s^{-1}.[18] Meanwhile, the introduction of electron-withdrawing moieties (such as imide, amide, and cyano) into π-conjugated semiconductors can lower the lowest unoccupied molecular orbital (LUMO) energy levels, because the π^* energy of the electron-withdrawing unit is relatively close to the LUMO energy of the π-conjugated system, and these orbitals can mix efficiently, leading to stabilization of the LUMO.[19] This strategy can switch electron donors to electron acceptors in some typical systems, for example, rylene to rylene diimide.[20] Since Zhan et al. reported a perylene diimide polymer acceptor in 2007,[21] some electron acceptors based on fused rings such as rylene diimide have shown relatively good performance in fullerene-free PSCs.[11–17,22–28] However, typical fused rings usually have high planarity and suffer from strong aggregation, leading to the formation of large crystalline domains (e.g., typically on a micrometer scale for rylene diimides).[20] Such large crystalline domains in BHJ films lead to large phase separations, reduced exciton diffusion/separation efficiencies, and finally low PCEs of the PSCs.[29] Therefore, a design principle for fused ring–based electron acceptors is to restrict planarity and self-aggregation by introducing rigid out-of-plane side chains onto the fused rings.

Here, we report the design and synthesis of a novel electron acceptor (ITIC, **Scheme 1**) based on a bulky seven-ring fused core (indacenodithieno[3,2-b]thiophene, IT), end-capped with 2-(3-oxo-2,3-dihydroinden-1-ylidene)malononitrile (INCN) groups, and with four 4-hexylphenyl groups substituted on it. Each INCN has one carbonyl and two cyano groups, and these electron-withdrawing groups can downshift LUMO levels. The push–pull structure in ITIC can induce intramolecular charge transfer and extend absorption. Furthermore, the four rigid 4-hexylphenyl substituents out of the IT main plane can restrict molecular planarity, aggregation, and large phase separation in BHJ blend films. ITIC possesses strong and broad absorption, low LUMO and highest occupied molecular orbital (HOMO) energy levels, good electron transport ability, and good miscibility with polymer donors. PSCs based on the widely used polymer donor PTB7-TH (Scheme 1) and ITIC blends exhibit PCEs up to 6.8% without any post-treatment, which is a new record for fullerene-free PSCs. The PTB7-TH:ITIC-based PSCs exhibit even better performance than the control devices based on PTB7-TH:$PC_{61}BM$ (where $PC_{61}BM$ is [6,6]-phenyl-C_{61}-butyric acid methyl ester), and are very close in performance to devices based on PTB7-TH:$PC_{71}BM$.

Scheme 1 shows the synthetic route to ITIC by means of two facile reactions. The IT was lithiated and then quenched with dimethylformamide (DMF) to afford IT-CHO in 93% yield, followed by a straightforward reaction with INCN to afford ITIC.

Dr. Y. Z. Lin, Dr. Z.-G. Zhang, Dr. H. T. Bai, Prof. Y. F. Li, Prof. D. B. Zhu
Beijing National Laboratory for Molecular Sciences
CAS Key Laboratory of Organic Solids
Institute of Chemistry
Chinese Academy of Sciences
Beijing 100190, P. R. China
J. Y. Wang, Prof. X. W. Zhan
Department of Materials Science and Engineering
College of Engineering
Peking University
Beijing 100871, P. R. China
E-mail: xwzhan@pku.edu.cn
Dr. Y. Z. Lin, Dr. H. T. Bai
University of Chinese Academy of Sciences
Beijing 100049, P. R. China

DOI: 10.1002/adma.201404317

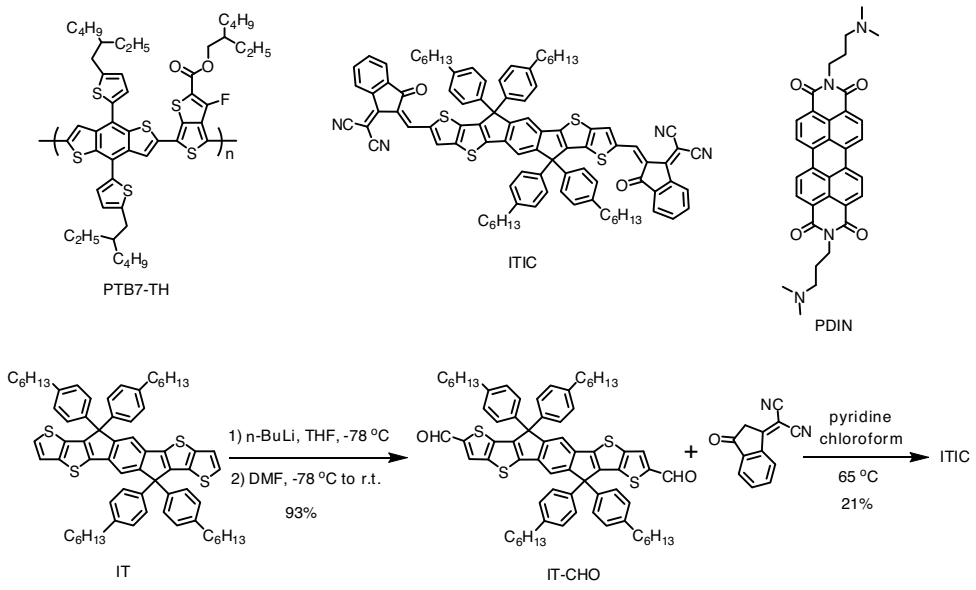

Scheme 1. Chemical structures of compounds PTB7-TH, ITIC, and PDIN, and synthetic route to ITIC.

The compound ITIC was fully characterized by matrix-assisted laser desorption ionization time-of-flight mass spectrometry (MALDI-TOF MS), ^{1}H NMR, ^{13}C NMR, and elemental analysis (Experimental Section). ITIC is readily soluble in common organic solvents such as chloroform and *o*-dichlorobenzene at room temperature because of its solubilizing alkyl substituents. This compound exhibits good thermal stability with a decomposition temperature (5% weight loss) at 345 °C in a nitrogen atmosphere, as measured by thermogravimetric analysis (TGA, Supporting Information (SI), Figure S1A). ITIC showed a small crystallization peak at 277 °C, measured by differential scanning calorimetry (DSC, SI, Figure S1B), indicating that it has weak crystallinity.

ITIC in dichloromethane solution (10^{-6} M) exhibits strong absorption in the 500–750 nm region with a maximum extinction coefficient of 1.3×10^5 M^{-1} cm^{-1} at 664 nm (**Figure 1**A). Relative to its solution, absorption of an ITIC film exhibits a significant redshift of 38 nm and a strong shoulder peak, suggesting that there is some molecular self-organization in the film. The optical bandgap of ITIC film estimated from the absorption edge (780 nm) is 1.59 eV. The electrochemical properties of ITIC were investigated by cyclic voltammetry (CV) with the ITIC film on a glassy carbon working electrode in 0.1 M $[n\text{-}Bu_4N]^+[PF_6]^-$ CH_3CN solution at a potential scan rate of 100 mV s^{-1}. ITIC exhibits irreversible reduction and quasi-reversible oxidation waves (Figure 1B). The onset oxidation and reduction potentials versus $FeCp_2^{+/0}$ (0.46 V) are 0.68 and –0.97 V, respectively; thus, the HOMO and LUMO energies are estimated to be –5.48 and –3.83 eV from the onset oxidation and reduction potentials, respectively, assuming the absolute energy level of $FeCp_2^{+/0}$ to be 4.8 eV below vacuum.[30]

The electron mobility of ITIC was measured using the space-charge-limited current (SCLC) method with the device structure Al/ITIC/Al (SI, Figure S2). The ITIC film exhibits electron mobility of up to 3.0×10^{-4} cm^2 V^{-1} s^{-1}, and an average value for five devices is 2.6×10^{-4} cm^2 V^{-1} s^{-1}. This electron mobility is close to those (ca. 10^{-4}–10^{-2} cm^2 V^{-1} s^{-1})[7] of fullerene derivatives and ensures effective charge carrier transport to the electrodes.

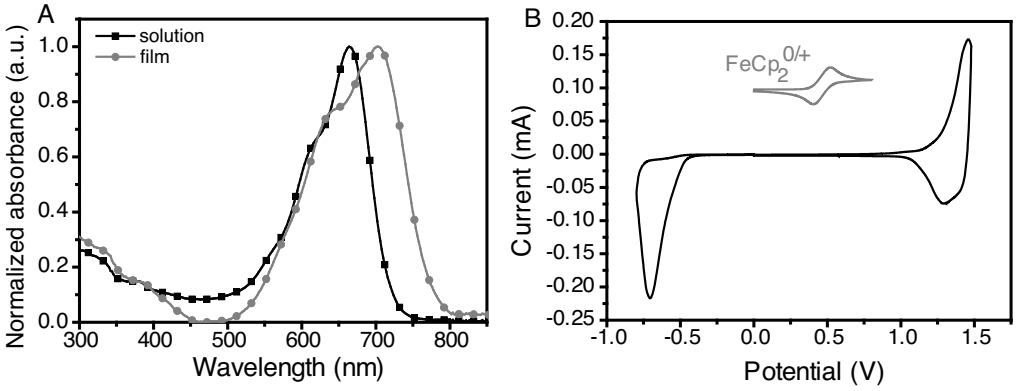

Figure 1. A) UV-vis absorption spectra of ITIC in dichloromethane solution and in thin film. B) Cyclic voltammogram for ITIC in CH_3CN/0.1 M $[n\text{-}Bu_4N]^+[PF_6]^-$ at 100 mV s^{-1}. The horizontal scale refers to a Ag/AgCl electrode.

Table 1. Device data (average PCEs in brackets) of PSCs based on PTB7-TH:ITIC under AM 1.5 G, 100 mW cm^{-2} illumination.

Donor:acceptor (w/w)	V_{OC} [V]	J_{SC} [mA cm^{-2}]	FF	PCE [%]
PTB7-TH:ITIC (1:1)	0.81	14.31	0.568	6.59 (6.46)
PTB7-TH:ITIC (1:1.3)	0.81	14.21	0.591	6.80 (6.58)
PTB7-TH:ITIC (1:1.5)	0.81	13.11	0.591	6.28 (6.21)
PTB7-TH:$PC_{61}BM$ (1:1.5)	0.83	11.94	0.611	6.05 (5.97)
PTB7-TH:$PC_{71}BM$ (1:1.5)	0.82	14.79	0.620	7.52 (7.29)

Chen and co-workers reported a promising low-bandgap polymer donor PTB7-TH (Scheme 1) based on benzodithiophene and thieno[3,4-b]thiophene units;[31] PTB7-TH exhibited a good hole mobility of 2.83×10^{-3} cm^2 V^{-1} s^{-1} measured by the SCLC method.[32] We used CV to estimate the energy levels of PTB7-TH. The LUMO of –3.59 eV and HOMO of –5.20 eV of PTB7-TH are 0.24 and 0.28 eV higher than those of ITIC (LUMO/HOMO: –3.83/–5.48 eV), respectively, and 0.24–0.28 eV is very close to the empirical value of 0.3 eV[33] required for efficient exciton dissociation. The gap between the LUMO of ITIC and the HOMO of PTB7-TH is as large as 1.37 eV, which could result in high open circuit voltage (V_{OC}) in solar cells. Blending PTB7-TH with ITIC results in over 97% fluorescence quenching of PTB7-TH and ITIC (SI, Figure S3), indicating that effective photoinduced charge transfer occurred between PTB7-TH and ITIC in the blended film and almost all excitons dissociated. This effective photoinduced charge transfer is beneficial to producing a high short-circuit current density (J_{SC}) in PSCs.

We used PTB7-TH as a donor and ITIC as an acceptor to fabricate BHJ PSCs with the structure ITO/PEDOT:PSS/PTB7-TH:ITIC/PDIN/Al, where ITO is indium tin oxide and PEDOT:PSS is poly(3,4-ethylenedioxythiophene)–poly(styrene sulfonate). PDIN (Scheme 1) serves as a cathode interlayer and can lower the work function of the electrode, allowing higher-work-function metals (such as Al) to act as the cathode,[34] similar to PEIE (polyethyleneimine ethoxylated).[35] **Table 1** summarizes V_{OC}, J_{SC}, fill factor (FF), and PCE of the devices at different donor/acceptor (D/A) weight ratios. The blend at a D/A weight ratio of 1:1.3 gave the best performance: V_{OC} of 0.81 V, J_{SC} of 14.21 mA cm^{-2}, FF of 0.591, and PCE of 6.80% (**Figure 2**A) with an average PCE of 6.58% for 30 devices. The PCEs > 6.5% are higher than those (4–5.7%) reported for fullerene-free PSCs; the amazing PCE of 6.80% is a new record for fullerene-free PSCs and can even compare favorably with typical fullerene-based PSCs. The control devices based on PTB7-TH:$PC_{61}BM$ or $PC_{71}BM$ showed a slightly higher V_{OC} of 0.82–0.83 V and FF of 0.61–0.62; the $PC_{61}BM$-based devices gave lower J_{SC} of 11.94 mA cm^{-2} and lower average PCE of 5.97%, and the $PC_{71}BM$-based devices gave slightly higher J_{SC} of 14.79 mA cm^{-2} and a better average PCE of 7.29%. The incident photon to converted current efficiency (IPCE) of the blended film with a PTB7-TH/ITIC weight ratio of 1:1.3 without any post-treatment is shown in Figure 2B. The blended film showed broad IPCE plateau spectra from 350 to 750 nm, with the IPCE maximum of 72.6% at 650 nm. The high IPCE from 550 to 750 nm corresponded to the strong absorption of PTB7-TH:ITIC (1: 1.3, w/w) blended film at 550–800 nm. Since the absorption spectra of PTB7-TH and ITIC are very similar and have strong overlap in the regions 300–400 nm and 500–800 nm, it was hard to differentiate their respective contributions to the photocurrent (Figure S4, SI). The calculated average J_{SC} was 14.02 mA cm^{-2}, similar to that measured by *J–V* measurements (1.3% mismatch).

The hole and electron mobilities of the blended films were measured using the SCLC method with the device structure ITO/PEDOT:PSS/PTB7-TH:ITIC (1:1.3)/Au for holes and Al/PTB7-TH:ITIC (1:1.3)/Al for electrons (SI, Figure S5). The blended film showed a hole mobility of 4.3×10^{-5} cm^2 V^{-1} s^{-1} and an electron mobility of 1.1×10^{-4} cm^2 V^{-1} s^{-1} with balanced charge transport ($\mu_e/\mu_h = 2.6$).

From atomic force microscopy (AFM) images (**Figure 3**A–D), PTB7-TH and ITIC have good miscibility with each other, and PTB7-TH:ITIC blended films show relatively smooth surfaces with a root-mean-square (RMS) roughness of 2.0 nm. The AFM phase image of the blend showed nearly uniform crystalline grains with phase-separation sizes around tens of nanometers estimated by cross-section profiles (Figure 3E), which approaches the exciton diffusion length in organic materials. The X-ray diffraction (XRD) data of the PTB7-TH:ITIC (1: 1.3, w/w) blend film showed two peaks, at 7.05° and 21.24°, suggesting ordered aggregation and π–π stacking (SI, Figure S6), which helps improve device performance.[36]

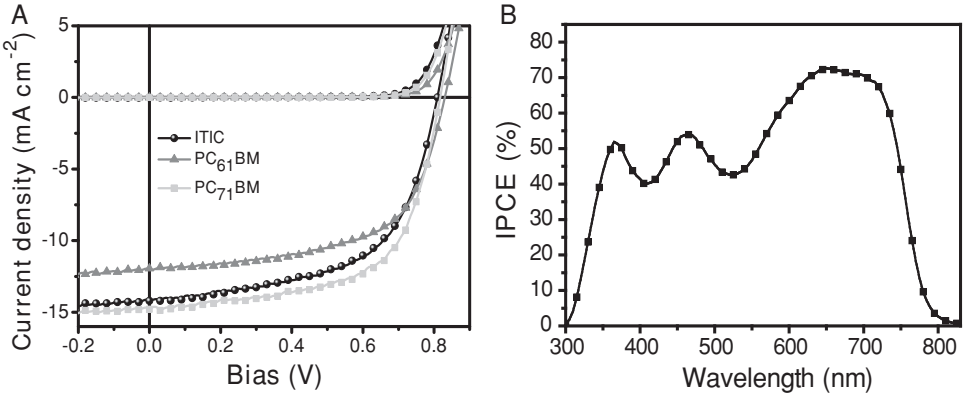

Figure 2. A) *J–V* curves of PSCs with the structure ITO/PEDOT:PSS/PTB7-TH:ITIC, $PC_{61}BM$ or $PC_{71}BM$/PDIN/Al. B) IPCE spectrum of a PTB7-TH:ITIC-based PSC.

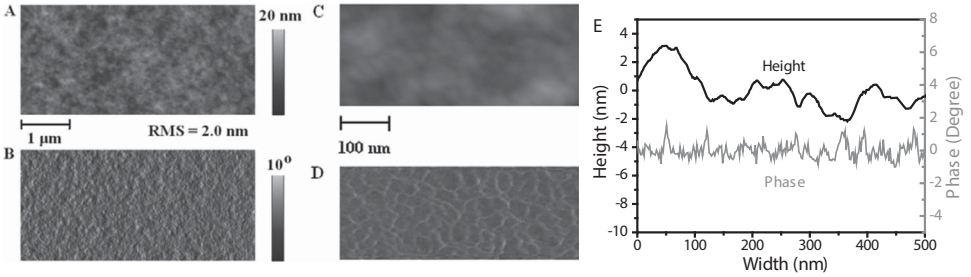

Figure 3. AFM height (A,C) and phase (B,D) images of PTB7-TH:ITIC blend film. E) Section curves.

Transmission electron microscopy (TEM) was used to investigate the internal structure of PTB7-TH:ITIC (1:1.3, w/w) blend film. The TEM image of the blend film (SI, Figure S7) revealed the crystalline grains, resembling the AFM images. These nanoscale crystalline domains are beneficial to charge separation and enhanced efficiency of the PSCs.

In summary, a novel electron acceptor (ITIC) based on a fused-ring core end-capped with INCN units has been designed and synthesized. ITIC exhibited a strong and broad absorption in the visible and even NIR regions, and appropriate energy levels matched with low-bandgap donor polymers such as PTB7-TH. Because of broad absorption, balanced charge transport, good donor/acceptor miscibility and proper phase-separation sizes of the blended film, PSCs based on PTB7-TH:ITIC blended films showed PCEs as high as 6.80%, which is a new reported record for fullerene-free PSCs,[37] and even higher than that (6.05%) of the control devices based on PTB7-TH:$PC_{61}BM$. These preliminary results demonstrate that the fused ring–based push–pull molecule ITIC is very promising as an alternative to fullerene derivatives for high-performance PSCs. We believe that this exciting result in fullerene-free PSCs can greatly promote the development of novel alternative acceptors for high-performance PSCs.

Experimental Section

Synthesis of IT-CHO: In a dry three-necked round-bottomed flask, compound IT (200 mg, 0.2 mmol) was dissolved in anhydrous THF (25 mL). The mixture was deoxygenated with argon for 30 min. At –78 °C, a solution of *n*-butyllithium (2.5 M in hexane, 0.19 mL, 0.48 mmol) was added dropwise. After 1 h of stirring at –78 °C, anhydrous DMF (0.04 mL) was added to this solution. The mixture was warmed to room temperature and stirred overnight. Brine (25 mL) was added and the mixture was extracted with chloroform (2 × 50 mL). The organic phase was dried over anhydrous $MgSO_4$ and filtered. After the solvent had been removed from the filtrate, the residue was purified by column chromatography on silica gel using petroleum ether/dichloromethane (1:1) as eluent, yielding a yellow solid (200 mg, 93%). ^{1}H NMR (400 MHz, $CDCl_3$): δ 9.89 (s, 2H), 7.94 (s, 2H), 7.62 (s, 2H), 7.16 (d, J = 8.4 Hz, 8H), 7.11 (d, J = 8.4 Hz, 8H), 2.58 (t, J = 7.6 Hz, 8H), 1.66 (m, 8H), 1.31 (m, 24H), 0.89 (m, 12H). ^{13}C NMR (100 MHz, $CDCl_3$): δ 182.89, 154.61, 149.50, 146.65, 144.40, 142.35, 141.77, 140.21, 139.21, 136.49, 129.86, 128.74, 127.84, 118.02, 63.12, 35.58, 31.70, 31.27, 29.14, 22.58, 14.10. MS (MALDI): m/z 1077 (M+1). Anal.: Calc. for $C_{70}H_{74}O_2S_4$: C, 78.17; H, 6.93. Found: C, 78.05; H, 6.86%.

Synthesis of ITIC: To a three-necked round-bottomed flask were added IT-CHO (200 mg, 0.19 mmol), 1,1-dicyanomethylene-3-indanone (279 mg, 1.4 mmol), chloroform (50 mL), and pyridine (1 mL). The mixture was deoxygenated with nitrogen for 30 min and then refluxed for 12 h. After cooling to room temperature, the mixture was poured into methanol (200 mL) and filtered. The residue was purified by column chromatography on silica gel using petroleum ether/dichloromethane (1:1) as eluent, yielding a dark blue solid (57 mg, 21%). ^{1}H NMR (400 MHz, $CDCl_3$): δ 8.87 (s, 2H), 8.70 (d, J = 7.6 Hz, 2H), 8.22 (s, 2H), 7.93 (d, J = 6.4 Hz, 2H), 7.79 (m, 4H), 7.63 (s, 2H), 7.23 (d, J = 8.4 Hz, 8H), 7.15 (d, J = 8.4 Hz, 8H), 2.58 (m, 8H), 1.61 (m, 8H), 1.33 (m, 24H), 0.87 (m, 12H). ^{13}C NMR (100 MHz, $CDCl_3$): δ 188.18, 160.36, 155.65, 152.86, 147.65, 147.06, 143.64, 142.51, 140.02, 139.60, 138.94, 138.24, 136.95, 136.86, 135.19, 134.49, 128.87, 127.89, 125.32, 123.76, 122.73, 118.53, 114.63, 114.57, 69.38, 63.24, 35.61, 31.70, 31.27, 29.20, 22.59, 14.10. MS (MALDI): m/z 1427 (M+1). Anal.: Calc. for $C_{94}H_{82}N_4O_2S_4$: C, 79.07; H, 5.79; N, 3.92. Found: C, 78.93; H, 5.70; N, 3.85%.

Fabrication and Characterization of PSCs: PSCs were fabricated with the structure ITO/PEDOT:PSS/PTB7-TH:ITIC, $PC_{61}BM$ or $PC_{71}BM$/PDIN/Al. The patterned ITO glass (sheet resistance = 10 Ω □$^{-1}$) was precleaned in an ultrasonic bath of acetone and isopropyl alcohol, and treated in an ultraviolet–ozone chamber (Jelight Company, Irvine, CA) for 20 min. A thin layer (30 nm) of PEDOT:PSS (Baytron P, now Clevios VP AI 4083, from H. C. Starck, Leverkusen, Germany) was spin-coated onto the ITO glass and baked at 150 °C for 15 min. A solution (total of 25 mg mL^{-1}) of PTB7-TH:ITIC blend was subsequently spin-coated (1000 rpm) on the PEDOT:PSS layer to form a photosensitive layer (ca. 100 nm thick). The thickness of the photosensitive layer was measured using an Ambios Technology (Santa Cruz, CA) XP-2 profilometer. The methanol solution (0.2% acetic acid) of PDIN at a concentration of 1.5 mg mL^{-1} was deposited on the active layer at 3000 rpm for 30 s, giving a PDIN layer ca. 14 nm thick. An aluminum (ca. 50 nm) layer was subsequently evaporated onto the surface of the PDIN layer under vacuum (ca. 10^{-5} Pa) to form the negative electrode. The active area of the device was 4 mm^2. The J–V curve was measured with a computer-controlled Keithley (Cleveland, OH) 236 Source Measure Unit. A xenon lamp coupled with AM1.5 solar spectrum filters was used as the light source, and the optical power at the sample was 100 mW cm^{-2}. The light intensity of the solar simulator was calibrated using a standard silicon solar cell. The IPCE spectrum was measured using a Stanford Research Systems (Sunnyvale, CA) model SR830 DSP lock-in amplifier coupled with a WDG3 monochromator and 500 W xenon lamp.

Supporting Information

Supporting Information is available from the Wiley Online Library or from the author.

Acknowledgements

The authors thank the 973 Program (2011CB808401), the National Natural Science Foundation of China (91433114, 21025418,

51261130582), the Chinese Academy of Sciences and Capital Normal University for financial support.

Received: September 17, 2014
Revised: November 7, 2014
Published online: January 7, 2015

[1] G. Yu, J. Gao, J. C. Hummelen, F. Wudl, A. J. Heeger, *Science* **1995**, *270*, 1789.
[2] Y. Li, *Acc. Chem. Res.* **2012**, *45*, 723.
[3] R. Sondergaard, M. Hosel, D. Angmo, T. T. Larsen-Olsen, F. C. Krebs, *Mater. Today* **2012**, *15*, 36.
[4] Y. W. Su, S. C. Lan, K. H. Wei, *Mater. Today* **2012**, *15*, 554.
[5] Z. He, C. Zhong, S. Su, M. Xu, H. Wu, Y. Cao, *Nat. Photonics* **2012**, *6*, 593.
[6] J. B. You, L. T. Dou, K. Yoshimura, T. Kato, K. Ohya, T. Moriarty, K. Emery, C. C. Chen, J. Gao, G. Li, Y. Yang, *Nat. Commun.* **2013**, *4*, 1446.
[7] Y. He, Y. Li, *Phys. Chem. Chem. Phys.* **2011**, *13*, 1970.
[8] Y. Lin, Y. Li, X. Zhan, *Chem. Soc. Rev.* **2012**, *41*, 4245.
[9] Y. Lin, X. Zhan, *Mater. Horiz.* **2014**, *1*, 470.
[10] X. Guo, A. Facchetti, T. J. Marks, *Chem. Rev.* **2014**, *114*, 8943.
[11] P. E. Hartnett, A. Timalsina, H. S. S. R. Matte, N. Zhou, X. Guo, W. Zhao, A. Facchetti, R. P. H. Chang, M. C. Hersam, M. R. Wasielewski, T. J. Marks, *J. Am. Chem. Soc.* **2014**, *136*, 16345.
[12] Y. Zhong, M. T. Trinh, R. Chen, W. Wang, P. P. Khlyabich, B. Kumar, Q. Xu, C.-Y. Nam, M. Y. Sfeir, C. Black, M. L. Steigerwald, Y.-L. Loo, S. Xiao, F. Ng, X. Y. Zhu, C. Nuckolls, *J. Am. Chem. Soc.* **2014**, *136*, 15215.
[13] R. Shivanna, S. Shoaee, S. Dimitrov, S. K. Kandappa, S. Rajaram, J. R. Durrant, K. S. Narayan, *Energy Environ. Sci.* **2014**, *7*, 435.
[14] X. Zhang, Z. Lu, L. Ye, C. Zhan, J. Hou, S. Zhang, B. Jiang, Y. Zhao, J. Huang, S. Zhang, Y. Liu, Q. Shi, Y. Liu, J. Yao, *Adv. Mater.* **2013**, *25*, 5791.
[15] Y. Zang, C.-Z. Li, C.-C. Chueh, S. T. Williams, W. Jiang, Z.-H. Wang, J.-S. Yu, A. K. Y. Jen, *Adv. Mater.* **2014**, *26*, 5708.
[16] Y. Zhou, T. Kurosawa, W. Ma, Y. Guo, L. Fang, K. Vandewal, Y. Diao, C. Wang, Q. Yan, J. Reinspach, J. Mei, A. L. Appleton, G. I. Koleilat, Y. Gao, S. C. B. Mannsfeld, A. Salleo, H. Ade, D. Zhao, Z. Bao, *Adv. Mater.* **2014**, *26*, 3767.
[17] D. Mori, H. Benten, I. Okada, H. Ohkita, S. Ito, *Energy Environ. Sci.* **2014**, *7*, 2939.
[18] C. Wang, H. Dong, W. Hu, Y. Liu, D. Zhu, *Chem. Rev.* **2012**, *112*, 2208.
[19] J. E. Anthony, A. Facchetti, M. Heeney, S. R. Marder, X. Zhan, *Adv. Mater.* **2010**, *22*, 3876.
[20] X. Zhan, A. Facchetti, S. Barlow, T. J. Marks, M. A. Ratner, M. R. Wasielewski, S. R. Marder, *Adv. Mater.* **2011**, *23*, 268.
[21] X. Zhan, Z. Tan, B. Domercq, Z. An, X. Zhang, S. Barlow, Y. Li, D. Zhu, B. Kippelen, S. R. Marder, *J. Am. Chem. Soc.* **2007**, *129*, 7246.
[22] E. Zhou, J. Cong, K. Hashimoto, K. Tajima, *Adv. Mater.* **2013**, *25*, 6991.
[23] T. V. Pho, F. M. Toma, M. L. Chabinyc, F. Wudl, *Angew. Chem. Int. Ed.* **2013**, *52*, 1446.
[24] P. Cheng, L. Ye, X. Zhao, J. Hou, Y. Li, X. Zhan, *Energy Environ. Sci.* **2014**, *7*, 1351.
[25] N. Zhou, H. Lin, S. J. Lou, X. Yu, P. Guo, E. F. Manley, S. Loser, P. Hartnett, H. Huang, M. R. Wasielewski, L. X. Chen, R. P. H. Chang, A. Facchetti, T. J. Marks, *Adv. Energy Mater.* **2014**, *4*, 1300785.
[26] Y. Lin, Y. Wang, J. Wang, J. Hou, Y. Li, D. Zhu, X. Zhan, *Adv. Mater.* **2014**, *26*, 5137.
[27] Y. Lin, J. Wang, S. Dai, Y. Li, D. Zhu, X. Zhan, *Adv. Energy Mater.* **2014**, *4*, 1400420.
[28] T. Earmme, Y.-J. Hwang, N. M. Murari, S. Subramaniyan, S. A. Jenekhe, *J. Am. Chem. Soc.* **2013**, *135*, 14960.
[29] Y. Huang, E. J. Kramer, A. J. Heeger, G. C. Bazan, *Chem. Rev.* **2014**, *114*, 7006.
[30] J. Pommerehne, H. Vestweber, W. Guss, R. F. Mahrt, H. Bässler, M. Porsch, J. Daub, *Adv. Mater.* **1995**, *7*, 551.
[31] S. H. Liao, H. J. Jhuo, Y. S. Cheng, S. A. Chen, *Adv. Mater.* **2013**, *25*, 4766.
[32] C. Cui, W.-Y. Wong, Y. Li, *Energy Environ. Sci.* **2014**, *7*, 2276.
[33] D. Veldman, S. C. J. Meskers, R. A. J. Janssen, *Adv. Funct. Mater.* **2009**, *19*, 1939.
[34] Z.-G. Zhang, B. Qi, Z. Jin, D. Chi, Z. Qi, Y. Li, J. Wang, *Energy Environ. Sci.* **2014**, *7*, 1966.
[35] Y. H. Zhou, C. Fuentes-Hernandez, J. Shim, J. Meyer, A. J. Giordano, H. Li, P. Winget, T. Papadopoulos, H. Cheun, J. Kim, M. Fenoll, A. Dindar, W. Haske, E. Najafabadi, T. M. Khan, H. Sojoudi, S. Barlow, S. Graham, J.-L. Brédas, S. R. Marder, A. Kahn, B. Kippelen, *Science* **2012**, *336*, 327.
[36] M. Y. Chiu, U. S. Jeng, C. H. Su, K. S. Liang, K. H. Wei, *Adv. Mater.* **2008**, *20*, 2573.
[37] A. Facchetti, *Mater. Today* **2013**, *16*, 123.